

Migration of Tharsis volcanism on Mars caused by differential rotation of the lithosphere

Shijie Zhong

The two most striking surface features on Mars are the Tharsis Rise and the crustal dichotomy^{1,2}. The crustal dichotomy, an elevation difference of ~5 km between the southern highlands and the northern lowlands, is the oldest geological feature on Mars, and the Tharsis Rise is a vast volcanic construct in the equatorial region of the planet, near the dichotomy boundary. Tharsis volcanism was initiated in the southern highlands and the main volcanic centre subsequently migrated to its current location³⁻⁵, suggesting relative motion between the lithosphere and the underlying mantle. However, as a one-plate planet, Mars cannot have large-scale motion of the lithosphere according to the standard theory of stagnant-lid convection^{6,7}. Here I use three-dimensional spherical shell models of mantle convection to demonstrate that a unique mode of horizontal motion of the lithosphere, differential rotation, is readily excited for Mars by one-plume convection and lithospheric thickness variations. The suggested mechanism explains the temporal and spatial patterns of Tharsis volcanism and offers a path to a unified model for Tharsis rise and the crustal dichotomy, with implications for volcanism, tectonics and true polar wander on other one-plate planetary bodies.

The crustal dichotomy and Tharsis Rise were formed in the first thousand million years of the Martian geological history^{1,2,8} (Fig. 1). The crustal dichotomy, as a consequence of crustal thickness variations⁹, was formed in the pre-Noachian time^{1,2,8} (>4.1 Gyr ago) owing to either exogenic^{8,10,11} or endogenic¹²⁻¹⁵ mechanisms. The Tharsis Rise was mainly formed in the Noachian between 4.0 and 3.7 Gyr (ref. 16), most likely caused by decompression melting of mantle upwelling plumes^{17,18}, and it has been the centre of Martian tectonics and volcanism for the past 4.0 Gyr (refs 1,2).

Tharsis volcanism has two distinct features. First, the volcanism occurred predominately in the western hemisphere. This hemispheric asymmetry is similar to that for crustal dichotomy except that the symmetry axes are off by ~90°. This asymmetry in the volcanism may be explained by one-plume mantle convection that can be dynamically generated with either a weak asthenosphere^{12,15} or endothermic phase change¹⁸, although only the former is consistent with timescales for Tharsis volcanism¹⁵. The second feature is the migration of Tharsis volcanic centres and their final location near the dichotomy boundary. Analyses of tectonic structures, topography and gravity, and crustal magnetism³⁻⁵ indicate that Tharsis volcanism was initiated in the Thaumasia region of ~40° S in the Early Noachian (~4.0 Gyr) and the main volcanic centre had subsequently migrated to its current location by the end of the Noachian at a rate of ~10°–20° per 100 Myr (Fig. 1). If Tharsis volcanism is caused by a plume, the migration of the Tharsis centre by >40° would suggest a relative motion between the plume and lithosphere, similar to how a plume produces the

Hawaiian volcanic chain on the Earth. However, this inference is inconsistent with the standard theory of stagnant-lid convection for one-plate planets such as Mars in which large-scale plate motion was not thought to occur.

The goals of this study are to (1) explore the feasibility of large-scale horizontal plate motion for one-plate planets and (2) understand the dynamic evolution of Tharsis volcanism including its migration and final location at the dichotomy boundary, and its relation to the crustal dichotomy. I propose a new hypothesis: rotation of the lithosphere relative to the mantle, as a unique form of plate motion, is readily excited for one-plate planets and it explains the key aspects of Tharsis volcanism. Rotation of the lithosphere relative to the mantle is the only possible mode of plate motion for one-plate planets and it represents spherical harmonic degree-1 toroidal plate motion. This rotation exists in the Earth's plate motion¹⁹. Mantle convection studies show that owing to mode coupling, lateral variations in mantle viscosity are required to generate any toroidal plate motion¹⁹. However, generation of rotation of the lithosphere on the Earth is effective only when lithospheric thickness variations including continental keels are considered²⁰.

To test this hypothesis, I formulate three-dimensional spherical shell models of mantle convection^{20,21} that include two features: (1) one-plume convection with a weak asthenosphere and (2) lithospheric thickness variations. A weak asthenosphere is used to generate one-plume convection (see Fig. 2 caption and Supplementary Information, Table S1 for further model description and parameters)^{12,15}. Lithospheric thickness variations are expected for early Mars as a result of the formation of the crustal dichotomy. The crustal thickness for the southern highlands is ~26 km thicker than that for the northern lowlands²². If the thickened crust is caused by melting, through either one-plume convection^{12,14,15} or overturn of magma ocean residue¹³, the melt residue could be hundreds of kilometres thicker below the thickened crust, depending on the melting rate. Owing to de-volatilization effects, the viscosity of the melt residue may increase by a factor of several hundred^{23,24}. Although the high-viscosity melt residue may not affect the lithospheric response to surface loading (elastic thickness), it may influence mantle flow significantly by effectively thickening the lithosphere²⁰.

Constructing a precise melt residue model based on the present-day crust model is complicated by the poorly constrained crust-modifying processes²⁵ and melting rate¹³. I use a simplified melt residue structure that is represented by a hemispheric cap of 90° arc radius. The thickness of the melt residue is 260 km at the centre of the cap and decreases linearly to zero at its boundary. I also consider another model in which melt residue thins much more rapidly near its boundary to mimic the present-day crustal thickness variations (see Supplementary Information, Table S1).

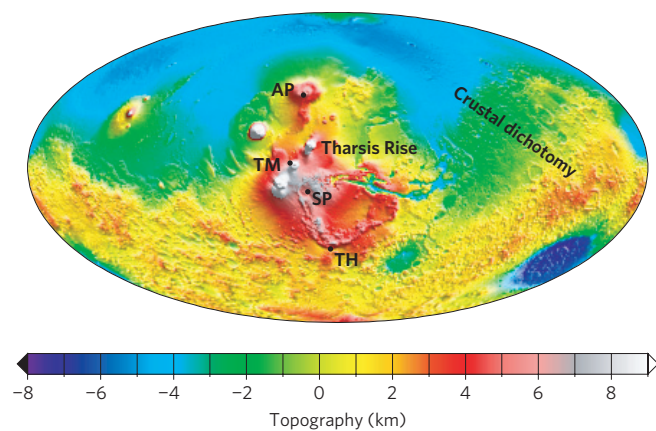


Figure 1 | Map of surface topography on Mars. This map shows the crustal dichotomy and the Tharsis Rise. TH, SP, TM and AP represent Thaumasia, Syria Planum, Tharsis Mons and Alba Patera, respectively.

The melt residue viscosity is taken to be 200 times the mantle background viscosity. Both the thickness and viscosity increase for the melt residue are consistent with those used for the Earth's continental keels^{20,23}.

Model 1 uses depth- and temperature-dependent viscosity for one-plume convection but does not include the melt residue (Fig. 3a). Model 1 is the same as the standard case for one-plume convection in an early study¹⁵ (also see Supplementary Information, Table S1). The initially small-scale structures evolve into one-plume convection that is dominated by a degree-1 component (Figs 2a,b and 3b), independent of initial conditions and convective vigour¹⁵. Once formed at a non-dimensional time of ~ 0.002 , the plume is stable with little horizontal migration (Fig. 3b). The lithospheric viscosity is about six orders of magnitude higher than that of the underlying asthenosphere (Fig. 3a), leading to stagnant-lid convection with negligibly small lithospheric motion (Fig. 3c).

Model 2 includes the high-viscosity melt residue and uses the temperature field in Fig. 2a from Model 1 as initial conditions, but otherwise is identical to Model 1. To minimize the effects of initial temperature, the melt residue cap is initially placed antipodal to the final one-plume structure from Model 1 (Fig. 2c). The melt residue cap, owing to its insulating effect, promotes upwelling plumes below the cap, and causes the formation of the one-plume structure there (Figs 2d, 3d). Previous numerical and laboratory studies have also shown that mantle plumes tend to develop below the thickened crust or lithosphere^{26,27}, but the lack of asthenosphere in these studies results in plumes also in other regions.

Rotation of the lithosphere is generated in Model 2 and becomes particularly strong after one-plume convection forms (Fig. 2d–f). The resulting plate motion is $\sim 20\%$ of the maximum mantle flow velocity (Fig. 3c). The lithosphere rotates at a rate of ~ 6 times that in the lower mantle but with opposite directions (Fig. 3e,f). For each depth layer, a rotation vector representing the rotation of the layer can be determined from the flow velocity, but the total rotation for the mantle and lithosphere must be zero in a non-rotating mantle reference frame²⁰. Comparison with Model 1 (Fig. 3c,e) indicates an important role of lateral variations in viscosity associated with the melt residue in exciting lithospheric rotation.

Rotation of the lithosphere relative to the mantle causes the angular separation between the centres of the plume and melt residue, $\Delta\theta$, to increase from $\sim 10^\circ$ when the one-plume structure is initially formed (Fig. 2d) to $\sim 90^\circ$ after a non-dimensional time of ~ 0.0017 (~ 300 Myr) to place the plume near the melt residue cap boundary (Figs 2f and 3d). The plume location is then stabilized with $\Delta\theta$ undulating around $\sim 90^\circ$ (Fig. 3d). The shear due to the

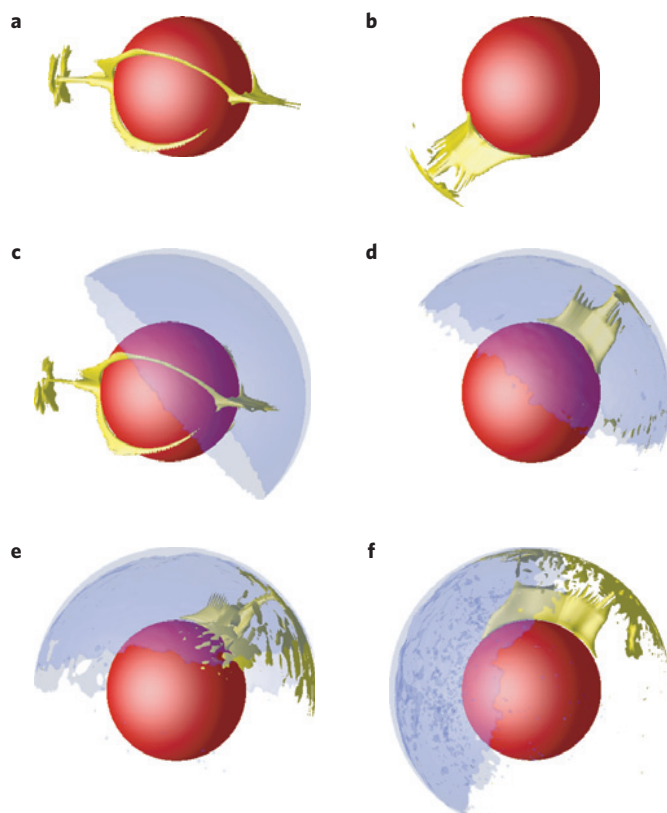


Figure 2 | Three-dimensional thermal structure from numerical models.

a–f, Snapshots of the thermal structure for Model 1 at non-dimensional times $t = 2.5 \times 10^{-4}$ (**a**) and 3.9×10^{-3} (**b**) and for Model 2 at $t = 2.6 \times 10^{-5}$ (**c**), 5.0×10^{-4} (**d**), 8.6×10^{-4} (**e**) and 2.05×10^{-3} (**f**). The red sphere, yellow isosurfaces and transparent, light-blue isosurfaces (only in **d–f**) represent the core, positive temperature anomalies and melt residue, respectively. The values for isosurfaces of thermal and melt residue structures are 0.07 and -0.1 , respectively. Model 1 is identical to case V3 in Roberts and Zhong¹⁵, which describes model formulation and parameters (see also Supplementary Information, Table S1).

rotation causes the lower mantle plume to elongate in the direction of relative motion, producing multiple plumes in the asthenosphere (Fig. 2f). This pattern of multiple plumes including their trending direction resembles that of Tharsis volcanism near the dichotomy (Fig. 1). Notice that the relatively small change in $\Delta\theta$ between times 0.001 and 0.0017 is caused by averaging multiple plumes in the asthenosphere (see Supplementary Information, Fig. S1).

Degree-1 core–mantle boundary (CMB) heat flux may have important effects on the early Martian dynamo²⁸. Surface heat flux due to mantle convection is significantly smaller in the hemisphere with thickened crust/melt residue owing to its insulating effect (Fig. 4a). It is often expected that the same hemisphere should have a higher mantle temperature and hence a smaller CMB heat flux, as in the early stage of Model 2 (see, for example, Fig. 2d). However, when the rotation of the lithosphere places the plume near the melt residue cap boundary (Fig. 2f), the hemisphere centred at the plume has a higher mantle temperature and a smaller CMB heat flux (Fig. 4b,c). The CMB heat flux exhibits significant variations with the maximum and minimum at about 84 and 0.1 mW m^{-2} , if scaled using appropriate parameters¹⁵. However, the degree-1 component of the CMB heat flux varies between 27 and 77 mW m^{-2} .

The basic results from Model 2 are found to be insensitive to model parameters and set-ups for the melt residue cap (see Supplementary Information, Fig. S2 for Model 3). Although Models

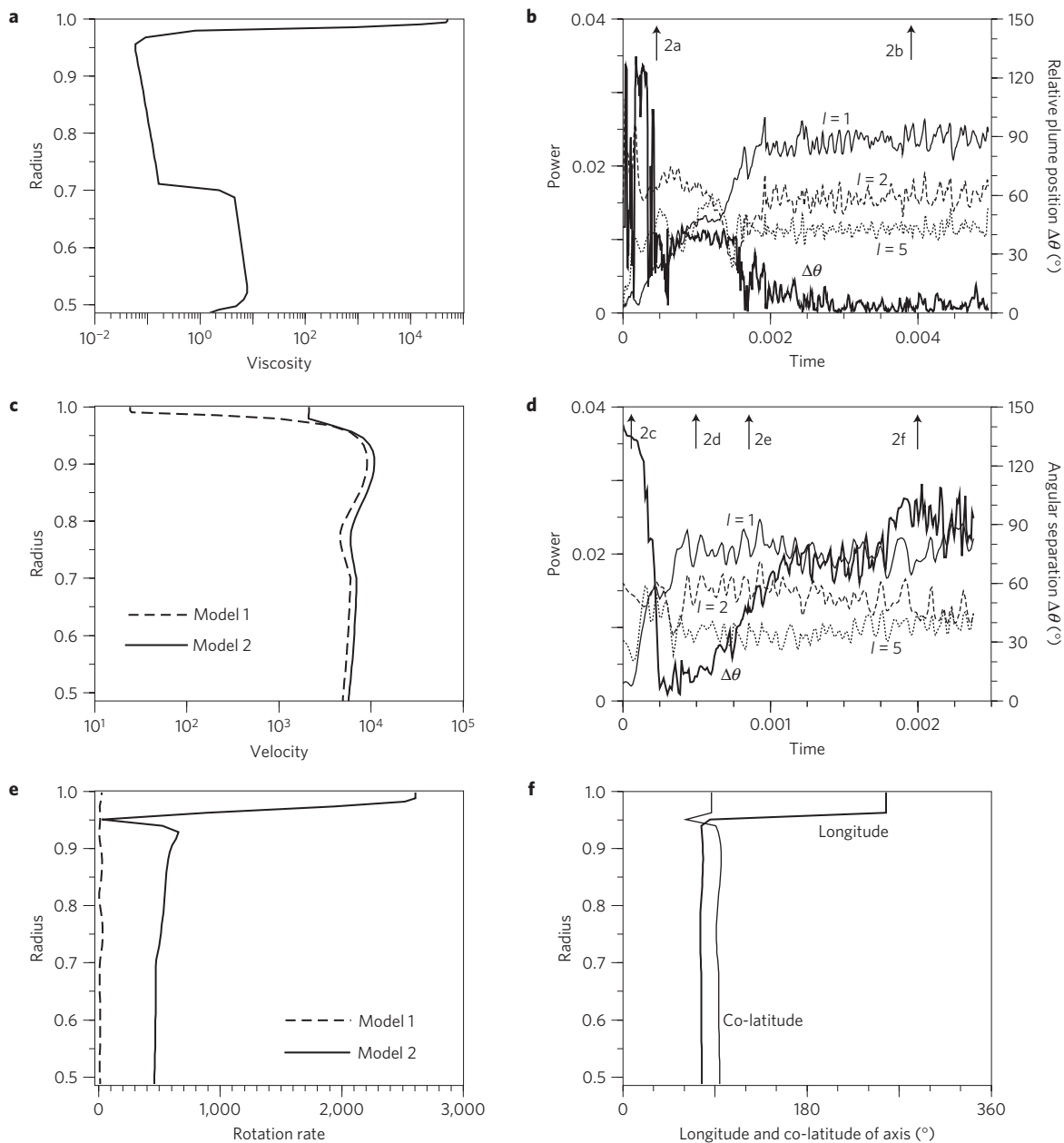


Figure 3 | Modelling results for spectra and flow velocity. **a**, Horizontally averaged viscosity from Model 1. **b**, Time-dependent spectra of the thermal structure at degrees 1, 2 and 5 near the CMB and the central position of the one-plume structure relative to its stable position for Model 1. **c**, Horizontally averaged flow velocity for Models 1 and 2 (corresponding to Fig. 2b,e). **d**, Time-dependent spectra and angular separation between the centres of the one-plume structure and of the melt residue, $\Delta\theta$, for Model 2. **e**, Depth-dependent rotation rates for Models 1 and 2 (corresponding to Fig. 2b,e). **f**, Directions of rotation axis for Model 2. The plume centre is determined by averaging the coordinates of nodal points at 540-km depth with high temperature. All of the quantities are non-dimensional¹⁵. With the parameters used here, a non-dimensional time of 10^{-3} and velocity of 10^3 are equivalent to ~ 170 Myr and 2 cm yr^{-1} , respectively¹⁵.

2 and 3 include large lithospheric thickness variations, edge-driven convection (small-scale convection driven by thermal anomalies associated with lithospheric thickness variations) that was speculated as a mechanism for Tharsis volcanism²⁹ is not observed. This suggests that edge-driven convection may require even sharper lithospheric thickness variations than in Models 2 and 3.

The rotation of the lithosphere relative to the mantle has implications for tectonics and volcanism on one-plate planets. First, the rotation of the lithosphere may complicate true polar wander (TPW) interpretation of surface features³⁰ such as deformation patterns related to the equatorial bulge, because the rotation may lead to similar features. Distinguishing between this rotation

and TPW is possible, but may not always be straightforward. Studies of TPW show that deforming the bulge requires energy and the TPW rate is limited by the bulge relaxation time and the size of the driving force³¹. With the relatively slow rate of the lithospheric rotation relevant to the migration of Tharsis volcanic centres, the bulge-deforming energy is ~ 3 orders smaller than that of mantle convection that drives the rotation of the lithosphere (see Supplementary Information, Note S1). Depending on the mantle viscosity, the bulge relaxation time may not pose a significant limit on the rotation of the lithosphere. Even in the limiting case of a lithosphere unable to rotate, differential motion between the plate and the underlying plume will still occur

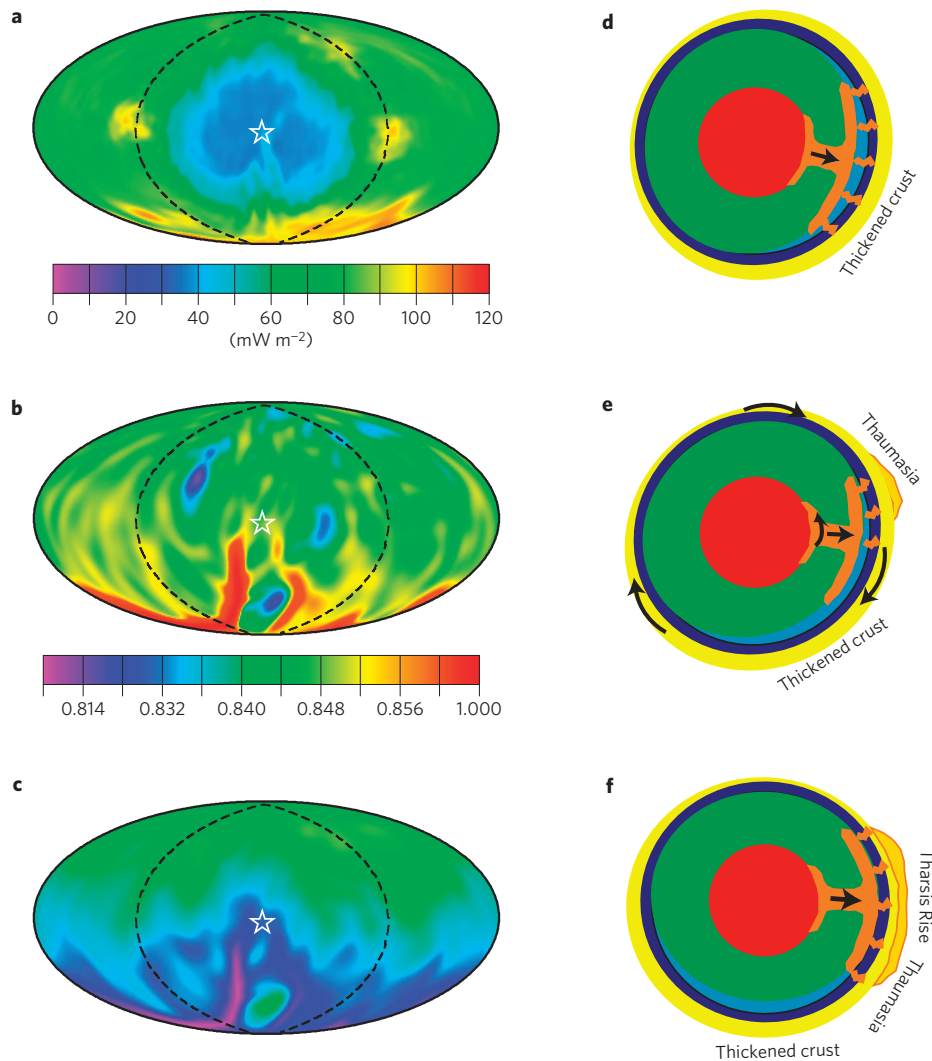


Figure 4 | Heat flux and a unified model. **a**, Surface heat flux. **b**, Non-dimensional temperature 160 km above the CMB. **c**, CMB heat flux for Model 2 at $t = 2.05 \times 10^{-3}$. **d-f**, Schematic descriptions of a unified model for the formation of the crustal dichotomy and Tharsis. The dashed line in **a-c** represents the melt residue cap with the star marking its centre. **a** and **c** use the same scale. The average CMB and surface heat fluxes are 52 and 72 mW m^{-2} with an internal heating rate of $\sim 82\%$. In **d-f**, the red, green, dark blue and yellow regions represent the core, mantle, lithospheric mantle and crust, respectively, and the light-blue region represents the melt residue.

(see Supplementary Information, Fig. S3 for Model 4), generating similar observational consequences to cases in which the rotation of the lithosphere occurs.

Second, for Mars, the rotation of the lithosphere offers a path to a unified model for the crustal dichotomy and Tharsis as summarized below. In the first stage, owing to either degree-1 convection or other mechanisms¹²⁻¹⁵, one-plume mantle flow develops, causing hemispherical scale melting and formation of a thickened crust (the crustal dichotomy) and melt residue in this hemisphere (Fig. 4d). The highly viscous melt residue interacts with either the original one-plume structure if it is generated from self-sustained degree-1 mantle convection^{12,15} or a new one-plume structure generated below the melt residue as in Model 2 if the original one-plume structure disappears because of its transient Rayleigh–Taylor instability^{13,14}, causing rotation of the lithosphere relative to the plume. When the plume is at Thaumasia in the Early Noachian, plume melting restarts possibly owing to thinner melt residue there, thus initiating the formation of Tharsis (Fig. 4e). As the rotation of the lithosphere continues to expose the lithosphere with ever thinner melt residue to the plume, significantly more melting is generated. The plume is eventually stabilized near

or slightly beyond the dichotomy boundary where lithospheric thickness is more uniform (Fig. 4f). This simple model may be tested with more realistic models that incorporate mantle melting and evolution of the crust and melt residue to enable direct comparison with observations.

Received 3 September 2008; accepted 18 November 2008; published online 14 December 2008

References

- Solomon, S. C. *et al.* New perspectives on ancient Mars. *Science* **307**, 1214–1220 (2005).
- Nimmo, F. & Tanaka, K. Early crustal evolution of Mars. *Annu. Rev. Earth Planet. Sci.* **33**, 133–161 (2005).
- Frey, H. V. Thaumasia: A fossilized early forming Tharsis uplift. *J. Geophys. Res.* **84**, 1009–1023 (1979).
- Mege, D. & Masson, P. A plume tectonics model for the Tharsis province, Mars. *Planet. Space Sci.* **44**, 1499–1546 (1996).
- Johnson, C. L. & Phillips, R. J. Evolution of the Tharsis regions of Mars: Insights from magnetic field observations. *Earth Planet. Sci. Lett.* **230**, 241–254 (2005).
- Head, J. W. & Solomon, S. C. Tectonic evolution of the terrestrial planets. *Science* **213**, 62–76 (1981).

7. Solomatov, V. S. Scaling of temperature- and stress-dependent viscosity convection. *Phys. Fluids* **7**, 266–274 (1995).
8. Frey, H. Impact constraints on, and a chronology for, major events in early Mars history. *J. Geophys. Res.* **111**, E08S91 (2006).
9. Zuber, M. T. *et al.* Internal structure and early thermal evolution of Mars from Mars Global Surveyor topography and gravity. *Science* **287**, 1788–1793.
10. Andrews-Hanna, J. C., Zuber, M. T. & Banerdt, W. B. The Borealis basin and the origin of the martian crustal dichotomy. *Nature* **453**, 1212–1215 (2008).
11. Nimmo, F., Hart, S. D., Korycansky, D. G. & Agnor, C. B. Implications of an impact origin for the martian hemispheric dichotomy. *Nature* **453**, 1220–1224 (2008).
12. Zhong, S. J. & Zuber, M. T. Degree-1 mantle convection and the crustal dichotomy on Mars. *Earth Planet. Sci. Lett.* **189**, 75–84 (2001).
13. Elkins-Tanton, L., Parmentier, E. M. & Hess, P. Possible formation of ancient crust on Mars through magma ocean processes. *J. Geophys. Res.* **110**, E12S01 (2005).
14. Ke, Y. & Solomatov, V. S. Early transient superplumes and the origin of the Martian crustal dichotomy. *J. Geophys. Res.* **110**, E10001 (2006).
15. Roberts, J. H. & Zhong, S. J. Degree-1 convection in the Martian mantle and the origin of the hemispheric dichotomy. *J. Geophys. Res.* **111**, E06013 (2006).
16. Phillips, R. J. *et al.* Ancient geodynamics and global-scale hydrology on Mars. *Science* **291**, 2587–2591 (2001).
17. Kiefer, W. S. Shergottite formation and implications for present-day Mantle convection on Mars. *Meteorit. Planet. Sci.* **38**, 1815–1832 (2003).
18. Harder, H. & Christensen, U. R. A one-plume model of Martian mantle convection. *Nature* **380**, 507–509 (1996).
19. Hager, B. H. & O'Connell, R. J. A simple global model of plate dynamics and mantle convection. *J. Geophys. Res.* **86**, 4843–4867 (1981).
20. Zhong, S. J. Role of ocean-continent contrast and continental keels on plate motion, net rotation of lithosphere and the geoid. *J. Geophys. Res.* **106**, 703–712 (2001).
21. McNamara, A. K. & Zhong, S. J. Thermochemical structures within a spherical mantle: Superplumes or piles? *J. Geophys. Res.* **109**, B07402 (2004).
22. Neumann, G. A. *et al.* Crustal structure of Mars from gravity and topography. *J. Geophys. Res.* **109**, E08002 (2004).
23. Pollack, H. N. Cratonization and thermal evolution of the mantle. *Earth Planet. Sci. Lett.* **80**, 175–182 (1986).
24. King, S. D. Archean cratons and mantle dynamics. *Earth Planet. Sci. Lett.* **234**, 1–14 (2005).
25. Nimmo, F. Tectonic consequences of Martian dichotomy modification by lower crustal flow and erosion. *Geology* **33**, 533–536 (2005).
26. Wenzel, M. J., Manga, M. & Jellinek, A. M. Tharsis as a consequence of Mars' dichotomy and layered mantle. *Geophys. Res. Lett.* **31**, L04702 (2004).
27. Wullner, U. & Harder, H. Convection underneath a crust inhomogeneously enriched heat sources: Application to Martian mantle dynamics. *Phys. Earth Planet. Inter.* **109**, 129–150 (1998).
28. Stanley, S., Elkins-Tanton, L., Zuber, M. T. & Parmentier, E. M. Mars' paleomagnetic field as the result of a single-hemisphere dynamo. *Science* **321**, 1822–1825 (2008).
29. Redmond, H. L. & King, S. D. The crustal dichotomy and edge driven convection: A mechanism for tharsis rise volcanism? *Lunar Planet. Sci. Conf. XXXVI* 1960 (abstr.) (2005).
30. Perron, J. T., Mitrovica, J. X., Manga, M., Matsuyama, I. & Richards, M. A. Evidence for an ancient martian ocean in the topography of deformed shorelines. *Nature* **447**, 840–843 (2007).
31. Matsuyama, I., Nimmo, F. & Mitrovica, J. X. Reorientation of planets with lithospheres: The effect of elastic energy. *Icarus* **191**, 401–412 (2007).

Acknowledgements

The author would like to thank F. Nimmo for discussions on TPW and S. King for reviewing the manuscript. This work is supported by the NASA MFR programme and the David and Lucile Packard Foundation. CIG distributes the software CitcomS that is used in this study.

Additional information

Supplementary Information accompanies this paper on www.nature.com/naturegeoscience. Reprints and permissions information is available online at <http://npg.nature.com/reprintsandpermissions>.